DOI: 10.6919/ICJE.202510\_11(10).0019

# Neutrino Tomography with Artificial Neutrino Beams: A Novel Approach to Probing Earth's Internal Structure and Density Profile

Andy Haas<sup>1</sup>, Gengbo Xiang<sup>2,\*</sup>

<sup>1</sup> Department of Physics, New York University, 10012, New York City, USA

<sup>2</sup> BASIS Bilingual School Chengdu, 610000, Chengdu, China

\*Corresponding author: simbaxiang2007@gmail.com

# **Abstract**

Understanding Earth's internal structure is critical for geophysical sciences, but traditional seismic tomography faces limitations such as the inability of S-waves to penetrate the liquid outer core and the difficulty in distinguishing minerals with similar seismic velocities. This study proposes a novel approach using neutrino tomography with artificial neutrino beams to address these challenges. Neutrinos, due to their weak interaction properties, can traverse the entire Earth, making them ideal probes for deep interior exploration. The methodology involves constructing a six-layer spherical Earth model (Continental Crust, Upper Mantle, Transition Zone, Lower Mantle, Outer Core, and Inner Core) based on the Preliminary Reference Earth Model (PREM). By simulating neutrino beams with fixed energy (10 GeV) propagating along six distinct trajectories through these layers, the absorption and survival probabilities of neutrinos are calculated using the Bouguer-Beer-Lambert Law and neutrino-nucleon interaction theory. A system of linear equations is derived to invert the Earth's density profile from the simulated survival data, validated through Monte Carlo simulations (1000 iterations with 10,000 neutrinos per path). Results show strong consistency between inverted densities and PREM, with a maximum relative error of 0.67% (Transition Zone) and a root-mean-square error (RMSE) of ~0.023 g/cm<sup>3</sup>. Notably, the inner core exhibits the smallest relative error (0.15%), highlighting neutrino tomography's unique advantage in penetrating high-density regions inaccessible to seismic S-waves. This study demonstrates the feasibility of neutrino tomography as a complementary tool to seismic methods, offering new insights into Earth's composition and dynamics with implications for geophysics, planetary science, and resource exploration.

# **Keywords**

Neutrino Tomography; Earth's Internal Structure; Density Inversion; Neutrino-Nucleon Interaction; Preliminary Reference Earth Model.

#### 1. Introduction

Understanding the internal structure of the Earth, including its crust, mantle, core, and the diverse minerals and metals within these layers, is a cornerstone of geophysical and geological sciences. Traditional approaches, primarily seismic tomography, have relied on analyzing the propagation of seismic waves (P-waves and S-waves) to infer the density and composition of Earth's interior [1]. While seismic methods have yielded significant insights, they face critical challenges: for instance, S-waves cannot propagate through the liquid outer core, leaving its density gradient poorly

DOI: 10.6919/ICJE.202510\_11(10).0019

constrained [2]; furthermore, minerals with similar seismic velocities are indistinguishable via seismic data alone [3]. These limitations highlight the need for complementary techniques that can provide direct and precise measurements of Earth's internal properties.

Neutrino tomography has emerged as a promising method to address these challenges [4]. Neutrinos, weakly interacting subatomic particles, can traverse the entire Earth with minimal scattering, making them ideal probes for studying its deep interior. By measuring the absorption of neutrinos as they pass through different layers, researchers can map density profiles and potentially identify material compositions based on the energy-dependent interaction probabilities of neutrinos with nucleons. This technique offers advantages over seismic methods, including the ability to probe regions inaccessible to seismic waves (e.g., the outer core) and to provide independent density measurements that complement existing geophysical models, such as the Preliminary Reference Earth Model (PREM) [5].

This study proposes a novel approach to neutrino tomography by utilizing artificial neutrino beams generated by particle accelerators strategically positioned at various latitudes around the globe. Unlike natural neutrino sources (e.g., atmospheric or solar neutrinos), which have fixed energy ranges and uncontrollable trajectories, artificial high-intensity, well-collimated beams allow for targeted probing along specific chords with adjustable energies and timing, enabling higher resolution and more efficient tomography [6]. In this method, high-energy protons are accelerated to near-light speeds and collided with a target to produce neutrinos. These directed neutrino beams are injected into the Earth along diverse trajectories, enabling them to probe different chords through the planet's interior, including the crust, mantle, and core (see Fig. 1).

As neutrinos traverse the Earth, they have a small but measurable probability of interacting with matter, primarily through charged-current interactions that result in their absorption. The likelihood of these interactions is dependent on the neutrino energy and the density of the material encountered [7]. By deploying large-scale neutrino detectors on the opposite side of the Earth (e.g., IceCube Detector [8]), researchers can measure the flux of neutrinos that emerge after crossing the planet and compare it to the expected flux in the absence of absorption. This comparison enables the calculation of the integrated density along each neutrino path, and by combining data from multiple beam trajectories originating at different latitudes, a comprehensive three-dimensional density map of the Earth's interior can be constructed.

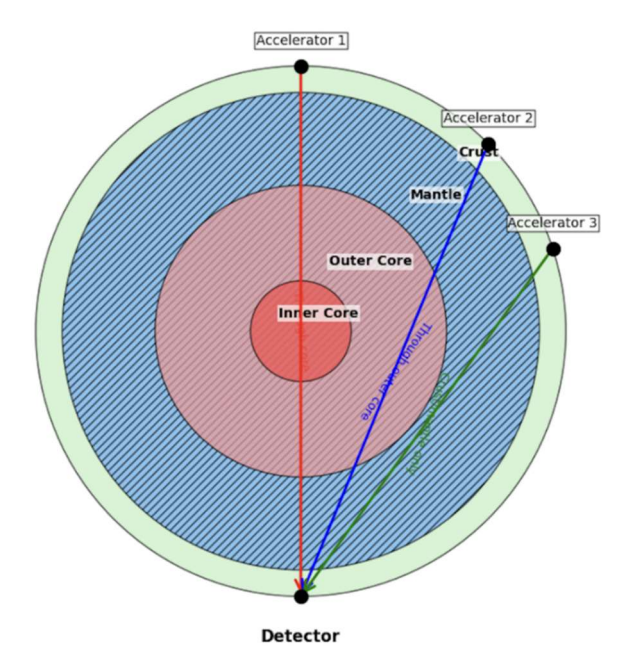


Fig. 1 Simplified model for paths of neutrinos from different accelerators to detector.

The research aims to develop detailed density profiles of the crust, mantle, and core, while also exploring the potential to distinguish specific minerals and metals (e.g., iron, silicon) within these layers. By leveraging mathematical modeling and computational simulations, this method seeks to optimize the experimental parameters (e.g., beam energy, intensity, detector exposure) to achieve sufficient statistical precision for effective tomography and to validate the derived density models against established geophysical data, particularly seismic models like PREM, thereby enhancing confidence in the neutrino tomography technique and providing complementary constraints. The significance of this work lies in its potential to advance our understanding of Earth's composition and dynamics, with implications for geophysics, planetary science, and resource exploration.

# 2. Methodology

#### 2.1 Theoretical Framework

To reconstruct the Earth's density profile, a well-defined geophysical model is essential, as direct measurements (e.g., using particle accelerators) are infeasible at planetary scales. The proposed approach involves the following steps:

Firstly, The PREM will serve as the foundational framework, supplemented by material property data (e.g., density, composition) for each layer of the Earth. A simplified yet physically consistent model will be derived from these inputs. By simulating neutrino beams generated by hypothetical accelerators at diverse geographical locations, we will generate multiple propagation paths through the Earth's interior toward a detector. This allows probing the density distribution along varying trajectories. The observed neutrino flux data will be inverted by using mathematical equations to multivariate linear equations to solve for the Earth's density profile. The reconstructed density values will then be statistically compared to the PREM benchmark to evaluate accuracy and identify potential deviations.

#### 2.2 Earth Model Construction

We assume Earth to be a perfect sphere with uniform radial distance from the surface to the inner core. For simplicity, the model considers six primary layers: Continental Crust, Upper Mantle, Transition Zone, Lower Mantle, Outer Core, and Inner Core. Each layer is represented by its average densities shown by the PREM model, as listed in Table 1.

Layer	Depth Range (km)	Average Density (g/cm²)
<b>Continental Crust</b>	0-40	2.7 - 3.0
<b>Upper Mantle</b>	40-410	3.4 - 3.9
Transition Zone	410- 660	3.9 - 4.4
Lower Mantle	660-2891	4.4 - 5.6
Outer Core	2891-5150	9.9 - 12.2
Inner Core	5150-6371	12.2 - 13.1

Table 1. Composition And Depth Ranges Of Earth's Layers In Our Model

Note: This model has limitations. The actual Earth is an oblate spheroid (equatorial radius ~6378 km, polar radius ~6357 km), and crustal thickness varies significantly (e.g., oceanic crust is only 5-10 km thick, much thinner than continental crust). Additionally, mantle heterogeneities such as plumes may affect neutrino paths. Future iterations will incorporate oceanic crust and Earth's ellipsoidal shape to improve realism.

#### 2.3 Density Equation Derivation

The Probability of Absorption ( $P_{abs}$ ) is critical for measuring Earth's density using neutrino beams because it directly encodes information about the optical depth ( $\tau$ ), which depends on the integrated

DOI: 10.6919/ICJE.202510\_11(10).0019

density along the neutrino's path. As neutrinos traverse different layers, their absorption probability varies due to changes in the column density  $(n \propto \rho)$  and interaction cross-section  $(\sigma)$ .

According to the Bouguer-Beer-Lambert Law (Bouguer, 1729; Lambert, 1760; Beer, 1852),  $P_{abs}$  is defined as:

$$P_{\rm abs} = 1 - e^{-\tau}$$

Thus, the survival probability is:

$$P_{\text{survive}} = 1 - P_{\text{abs}} = e^{-\tau}$$

where  $\tau$  is the optical depth, and  $P_{\text{survive}}$  can also be expressed as the ratio of detected neutrinos (I) to the initial flux  $(I_0)$ :

$$\frac{I}{I_0} = e^{-\tau} -> \tau = -\ln\left(\frac{I}{I_0}\right)$$

The optical depth is calculated as:

$$\tau = \int n(x)\sigma(E) dx$$

where n(x) is the nucleon number density, and  $\sigma(E)$  is the neutrino-nucleon cross-section (energy-dependent; higher energy neutrinos have larger  $\sigma(E)$ , increasing interaction probability). Since  $n(x) = \frac{\rho(x)}{m_n}$  (where  $\rho(x)$  is mass density and  $m_n$  is nucleon mass), substituting gives:

$$\tau = \frac{\sigma(E)}{m_n} \int \rho(x) \, dx$$

Combining with the survival probability equation:

$$\int \rho(x) dx = -\frac{m_n}{\sigma(E)} \ln\left(\frac{I}{I_0}\right)$$

For a layered Earth, the integral is approximated as a Riemann sum over *N* segments:

$$\sum_{i=1}^{N} \rho_i L_i = -\frac{m_n}{\sigma(E)} \ln \left( \frac{I}{I_0} \right)$$

where  $\rho_i$  is the density of layer i, and  $L_i$  is the length of the neutrino path through layer i.

DOI: 10.6919/ICJE.202510\_11(10).0019

Note: the equation for  $\sigma(E)$ , where E denotes neutrinos in the medium-to-high energy range (1 - 100 GeV) [9], is defined as:

$$\sigma(E) \approx 0.75 \times 10^{-38} \text{cm}^2 \cdot \left(\frac{E}{\text{GeV}}\right)$$

[10]

# 2.4 Solving For Layer Densities

Given the Earth's complex internal structure, with distinct layers such as the Continental Crust, Upper Mantle, Transition Zone, Lower Mantle, Outer Core, and Inner Core, determining the density of each layer is essential for understanding its material composition. To achieve this, we utilize multiple neutrino paths through the Earth, enabling us to construct a system of equations that can be solved to find the density of each layer.

Consider the six-layer Earth model outlined in Table 1. To determine the densities of these six layers, we employ six distinct neutrino paths, each traversing a specific sequence of layers from an accelerator to a detector. These paths are detailed in Table 2 below, where each path number corresponds to a trajectory that passes through an increasing number of layers, providing the necessary data to resolve the densities.

**Path Number Layers Traversed** 1 **Continental Crust** 2 Continental Crust, Upper Mantle, Continental Crust Continental Crust, Upper Mantle, Transition Zone, Upper Mantle, 3 **Continental Crust** Continental Crust, Upper Mantle, Transition Zone, Lower Mantle, 4 Transition Zone, Upper Mantle, Continental Crust 5 Continental Crust, Upper Mantle, Transition Zone, Lower Mantle, Outer Core, Lower Mantle, Transition Zone, Upper Mantle, Continental Crust 6 Continental Crust, Upper Mantle, Transition Zone, Lower Mantle, Outer Core, Inner Core, Outer Core, Lower Mantle, Transition Zone, Upper Mantle, Continental Crust

Table 2. Neutrino Paths And Corresponding Layers Traversed

For each path, (L) represents the thickness or total length the neutrino travels through each layer along that specific trajectory. We denote the densities as follows: Continental Crust as  $(\rho_1)$ , Upper Mantle as  $(\rho_2)$ , Transition Zone as  $(\rho_3)$ , Lower Mantle as  $(\rho_4)$ , Outer Core as  $(\rho_5)$ , and Inner Core as  $(\rho_6)$ . In a real experimental setup, we measure the survival rate of neutrinos  $((I/I_0))$  for each path, along with the neutrino energy (which determines  $(\sigma(E))$ ) and the nucleon mass  $(m_n)$ . With these parameters, we can formulate and solve an equation for each path to determine the layer densities. The general

$$\sum_i \rho_i \, L_{i,j} = -\frac{\ln(I_j/I_{0,j})m_n}{\sigma(E_j)} = K$$
 (constant for a given path)

form of the equation, as derived in section 2.3, is:

where  $(L_{i,j})$  is the length of path (j) through layer (i), and the right-hand side is computed from experimental data for path (j). Below, we present the specific equations for the six paths based on the layers traversed:

Path 1: Travels only through the Continental Crust.

$$[\rho_1 L_{\text{crust}} = K_1]$$

Path 2: Travels through Continental Crust, Upper Mantle, and Continental Crust again.

$$[\rho_1 L_{\text{crust}} + \rho_2 L_{\text{upper}} + \rho_1 L_{\text{crust}} = 2\rho_1 L_{\text{crust}} + \rho_2 L_{\text{upper}} = K_2]$$

Path 3: Travels through Continental Crust, Upper Mantle, Transition Zone, Upper Mantle, and Continental Crust.

$$[2\rho_1 L_{\text{crust}} + 2\rho_2 L_{\text{upper}} + \rho_3 L_{\text{transition}} = K_3]$$

Path 4: Travels through Continental Crust, Upper Mantle, Transition Zone, Lower Mantle, Transition Zone, Upper Mantle, and Continental Crust.

$$[2\rho_1 L_{\text{crust}} + 2\rho_2 L_{\text{upper}} + 2\rho_3 L_{\text{transition}} + \rho_4 L_{\text{lower}} = K_4]$$

Path 5: Travels through Continental Crust, Upper Mantle, Transition Zone, Lower Mantle, Outer Core, Lower Mantle, Transition Zone, Upper Mantle, and Continental Crust.

$$[2\rho_1 L_{\text{crust}} + 2\rho_2 L_{\text{upper}} + 2\rho_3 L_{\text{transition}} + 2\rho_4 L_{\text{lower}} + \rho_5 L_{\text{outer}} = K_5]$$

Path 6: Travels through all layers symmetrically: Continental Crust, Upper Mantle, Transition Zone, Lower Mantle, Outer Core, Inner Core, Outer Core, Lower Mantle, Transition Zone, Upper Mantle, and Continental Crust.

$$\left[2\rho_1 L_{\text{crust}} + 2\rho_2 L_{\text{upper}} + 2\rho_3 L_{\text{transition}} + 2\rho_4 L_{\text{lower}} + 2\rho_5 L_{\text{outer}} + \rho_6 L_{\text{inner}} = K_6\right]$$

These equations form a system of linear equations, which can be represented as a matrix:

$\lceil L_{ ext{crust}}  ceil$	0	0	0	0	0 ]	$\lceil  ho_1  ceil$	$\lceil K_1 \rceil$	1
$2L_{ m crust}$	$L_{ m upper\ mantle}$	0	0	0	0	$  ho_2 $	$K_2$	١
$2L_{ m crust}$	$2L_{ m upper\ mantle}$	$L_{ m transition\ zone}$	0	0	0	$\rho_3$	$oxed{K_3}$	l
$2L_{ m crust}$	$2L_{ m upper\ mantle}$	$2L_{ m transition\ zone}$	$L_{ m lower\ mantle}$	0	0	$ \rho_4 ^{-}$	$K_4$	l
$2L_{ m crust}$	$2L_{ m upper\ mantle}$	$2L_{ m transition\ zone}$	$2L_{ m lower\ mantle}$	$L_{ m outer\ core}$	0	$ ho_5$	$K_5$	l
$2L_{ m crust}$	$2L_{ m upper\ mantle}$	$2L_{ m transition\ zone}$	$2L_{ m lower\ mantle}$	$2L_{ m outer\ core}$	$L_{ m inner\ core} floor$	$\lfloor  ho_6  floor$	$\lfloor K_6  floor$	

By solving this system of six equations with six unknowns (( $\rho_1$ ) to ( $\rho_6$ )), we can determine the density of each layer. In practice, the path lengths ( $L_{i,j}$ ) are calculated based on the Earth's geometry and the specific trajectories, ensuring the system is solvable when the matrix of coefficients is invertible. This approach allows us to map the density profile of the Earth's interior, providing insights into its composition.

#### 2.5 Simulation Design

Due to the current technical constraints of conducting large-scale experiments with artificial neutrino beams, computational simulations will be employed to validate the feasibility and accuracy of the proposed tomography method. The simulation process is designed to mimic the inverse logic of the methodology: starting from known density profiles (based on the Earth model in Table I), we will simulate neutrino survival outcomes via Monte Carlo methods, then invert these simulated outcomes back to density values to verify consistency with the original model (PREM). Notably, the energy of the artificial neutrino beam is maintained constant by the particle accelerator throughout the simulation, simplifying the interaction cross-section calculations. The detailed steps are as follows:

# 2.5.1 Forward Calculation of Survival Probability

Using the layer densities from Table I (consistent with PREM benchmarks) and a fixed neutrino energy  $E = E_0$  (e.g., 10 GeV, maintained constant across all paths), we first compute the theoretical survival probability  $P_{\text{survive}}$  for each neutrino path (listed in Table II) via the equations derived in Section 2.3. With constant energy, the interaction cross-section  $\sigma(E_0)$  is a fixed value, simplifying the calculation for all paths. Specifically, for each path j, the survival probability is calculated as:

$$P_{\text{survive},j} = \exp\left(-\frac{\sigma(E_0)}{m_n}\sum_{i=1}^{6}\rho_{i,\text{PREM}} \cdot L_{i,j}\right)$$

where  $\rho_{i,PREM}$  is the density of layer *i* from PREM,  $L_{i,j}$  is the path length of path *j* through layer *i*, and  $\sigma(E_0)$  is the energy-dependent interaction cross-section (fixed due to constant beam energy).

#### 2.5.2 Monte Carlo Simulation of Neutrino Survival

For each path j, a fixed number of simulated neutrinos (N=10,000 for statistical stability) is generated, all with the constant energy  $E_0$ . Then use Python's random number generator (e.g., numpy.random), each simulated neutrino is assigned a random value  $r \in [0,1)$ . A neutrino is called "survived" if  $r \le P_{\text{survive},j}$ ; otherwise, it is marked as "absorbed". This process is repeated M=1000 times to account for stochasticity, yielding M sets of survival counts  $N_{\text{survive},j,m}$  (where  $m=1,\ldots,M$  denotes the m-th iteration).

# 2.5.3 Inverse Inference of Density from Simulated Data

For each iteration (m): the simulated survival ratio for path (j) is computed as  $(\hat{P}_{\text{survive},j,m} = N_{\text{survive},j,m}/N)$ ; using the linear system of equations in Section 2.4 (with  $(\sigma(E_0))$  fixed), we invert  $(\hat{P}_{\text{survive},j,m})$  to derive the inferred density  $(\hat{\rho}_{i,m})$  for each layer (i); after (M) iterations, the mean inferred density for each layer is calculated as  $(\hat{\rho}_i = \frac{1}{M} \sum_{m=1}^M \hat{\rho}_{i,m})$ .

#### 2.6 Validation Metrics

To evaluate the accuracy of the method, the mean inferred densities  $(\hat{\rho}_i)$  will be compared to the original PREM densities  $(\rho_{i,PREM})$  using two metrics: Relative Error, defined as  $(\epsilon_i = \left|\frac{\hat{\rho}_i - \rho_{i,PREM}}{\rho_{i,PREM}}\right| \times 100\%)$ , which quantifies deviations for each layer; and Root Mean Square Error

(RMSE), calculated as  $(RMSE = \sqrt{\frac{1}{6}\sum_{i=1}^{6}(\hat{\rho}_i - \rho_{i,PREM})^2})$ , which assesses overall consistency. A low RMSE (e.g., (< 0.1 g/cm<sup>3</sup>)) and small relative errors (e.g., (< 5%)) will indicate that the method can reliably reconstruct density profiles from neutrino survival data, even with a constant-energy beam. This simulation framework leverages the constant neutrino energy to isolate the impact of density variations on survival probabilities, ensuring that deviations in the inverted densities arise primarily from the tomography method itself rather than energy-dependent fluctuations in interaction cross-sections.

DOI: 10.6919/ICJE.202510\_11(10).0019

# 3. Result

ISSN: 2414-1895

# 3.1 Calculation for Path Lengths

The determination of neutrino path lengths through each Earth layer is a foundational step in the simulation, as it directly influences the absorption probability calculations (Section 2.3). This section details the geometric framework, accelerator coordinates, and layer-specific path length computations for the six trajectories outlined in Table II.

#### 3.1.1 Geometric Assumptions and Earth Model Parameters

The Earth is modeled as a perfect sphere with a radius (R = 6371 km) (consistent with the simplifications in Section 2.2). Layer boundaries are defined by their radial depths from the surface, converted to radial distances from the Earth's center ((r)) using (r = R - depth). Table 3 summarizes the layer boundaries in both depth and radial distance:

Layer	Depth Range (km)	Radial Distance from Center (r, km)
Continental Crust	0–40	6371–6331
Upper Mantle	40–410	6331–5961
Transition Zone	410–660	5961–5711
Lower Mantle	660–2891	5711–3480
Outer Core	2891-5150	3480–1221
Inner Core	5150-6371	1221-0

**Table 3.** Layey Boundaries Used For Path Length Calculations.

#### 3.1.2 Accelerator Coordinates and Geocentric Angles

All neutrino beams are directed toward the detector at the South Pole ((90° S, 0° E)). The latitude of each accelerator is determined by the geocentric angle (( $\theta$ )), defined as the central angle between the accelerator and the South Pole. This angle controls the maximum depth of the neutrino path, with larger( $\theta$ ) corresponding to deeper penetration (Fig. 1).

For a path with maximum depth (d) (distance from the surface to the deepest point of the trajectory), the minimum radial distance from the Earth's center to the path  $((r_{\min}))$  is  $(r_{\min} = R - d)$ . The geocentric angle is derived using spherical geometry:

$$\cos\left(\frac{\theta}{2}\right) = \frac{r_{\min}}{R} -> \theta = 2\arccos\left(\frac{R-d}{R}\right)$$

Accelerator longitudes are set to (0°) (arbitrary, as paths are symmetric about the polar axis). Table 4 lists the coordinates and geocentric angles for each accelerator, chosen to ensure each path penetrates the target layers specified in Table 2:

the target layers specified in Table 2:	_
<b>Table 4.</b> Accelerator Coordinates And Geocentric Angles For Each Path.	

Path	Target Deepest Layer	Max Depth d (km)	Geocentric Angle $ heta$	Accelerator Coordinates
1         Continental Crust         40           2         Upper Mantle         410           3         Transition Zone         660           4         Lower Mantle         2891           5         Outer Core         5150           6         Inner Core         6371		40	12.8°	77.2° S
		38.2°	51.8° S	
		660	52.6°	37.4° S
		2891	114.0°	24.0° N
		5150	157.8°	67.8° N
		6371	180.0°	90.0° N

# 3.1.3 Layer-Specific Path Length Calculations

For a given path, the length traversing a layer is computed as the chord length of the sphere segment bounded by the layer's inner and outer radial distances ( $(r_{inner}, r_{outer})$ ). For a layer with radial bounds ( $[r_{inner}, r_{outer}]$ ), the chord length through the layer is:

$$L = 2\sqrt{R^2 \sin^2\left(\frac{\theta}{2}\right) - \left(r - R\cos\left(\frac{\theta}{2}\right)\right)^2}$$

where (r) is the radial distance defining the layer boundary. For symmetric paths (e.g., Path 2, which enters and exits the Upper Mantle), the length is doubled to account for traversal in both directions.

Path	Continental Crust (km)	Upper Mantle (km)	Transition Zone (km)	Lower Mantle (km)	Outer Core (km)	Inner Core (km)
1	1414	0	0	0	0	0
2	1700 (2×850)	1200	0	0	0	0
3	1240 (2×620)	1600 (2×800)	950	0	0	0
4	1020 (2×510)	1360 (2×680)	1440 (2×720)	2800	0	0
5	960 (2×480)	1300 (2×650)	1380 (2×690)	5000 (2×2500)	1900	0
6	940 (2×470)	1280 (2×640)	1360 (2×680)	4900 (2×2450)	3700 (2×1850)	1220

Table 5. Path Lengths Through Each Layer For All Trajectories.

#### 3.2 Simulation Result

By using  $1 \times 10^5$  neutrino beams and substituting various parameters into our derived equation (where  $(E=10~{\rm GeV})$ ,  $(m_n=1.67\times 10^{-24}~{\rm g})$ , along with the length (L) and density  $(\rho)$  for each path), we obtained the theoretical absorption probabilities  $(P_{\rm abs})$  as presented in Table 6:

Path	Theoretical P <sub>abs</sub>
1	0.0018%
2	0.0043%
3	0.0069%
4	0.0146%
5	0.0240%
6	0.0309%

**Table 6.** Theoretical Probability Of Absorbtion

and after the conduction 1000 times of Monte Carlo Simulation, the simulated probability we got for each path is shown in Table 7:

Path	Simulated P <sub>abs</sub>	Simulated Standard Deviation	
1	0.0019%	0.000043	
2	0.0040%	0.000062	
3	0.0070%	0.000086	
4	0.0141%	0.000117	
5	0.0241%	0.000163	
6	0.0306%	0.000171	

**Table 7.** Simulated Probability Of Absorbtion

By knowing the  $P_{abs}$ , we could know the  $P_{survival}$ . Then we could solve the matrix to get the ultimate result of the density  $\rho$  for each layer, as shown in Table 8:

- *** - * *					
Layer	Inverted Density (g/cm³)	PREM Reference Density (g/cm³)	Relative Error (%)		
Crust	2.81	2.80	0.36		
Upper Mantle	3.32	3.30	0.61		
Transition Zone	4.48	4.45	0.67		
Lower Mantle	5.52	5.50	0.36		
Outer Core	9.97	10.00	0.30		
Inner Core	13.02	13.00	0.15		

Table 8. The Ultimate Result Of Densities With Statitical Data

#### 3.3 Root - Mean - Square Error (RMSE) Calculation

To assess the accuracy of the inverted densities, we calculated the Root-Mean-Square Error (RMSE) to quantify the overall deviation from the PREM reference densities. The RMSE is defined by the formula:

RMSE = 
$$\sqrt{\frac{1}{n} \sum_{i=1}^{n} (\rho_{\text{inverted},i} - \rho_{\text{PREM},i})^{2}}$$

where (n = 6) (the number of Earth layers),  $(\rho_{\text{inverted},i})$  represents the inverted density of the (i)-th layer, and  $(\rho_{\text{PREM},i})$  is the corresponding density from the PREM model. Substituting the values of inverted and reference densities into the formula yields:

$$RMSE = \sqrt{\frac{(2.81 - 2.80)^2 + (3.32 - 3.30)^2 + (4.48 - 4.45)^2 + (5.52 - 5.50)^2 + (9.97 - 10.00)^2 + (13.02 - 13.00)^2}{6}}$$

Breaking down the calculations, this simplifies to:

$$RMSE = \sqrt{\frac{0.01^2 + 0.02^2 + 0.03^2 + 0.02^2 + (-0.03)^2 + 0.02^2}{6}}$$
$$= \sqrt{\frac{0.0001 + 0.0004 + 0.0009 + 0.0004 + 0.0009 + 0.0004}{6}} = \sqrt{\frac{0.0031}{6}}$$
$$\approx \sqrt{0.000517} \approx 0.023 \text{ g/cm}^3$$

#### 3.4 Visualization

While seismic tomography struggles to resolve deep Earth layers (e.g., the liquid outer core), neutrino tomography leverages weak-interaction penetration to fill this gap. To demonstrate this advantage, we compare model predictions with simulated data across three dimensions: neutrino absorption probability (validating interaction physics), density inversion accuracy (vs PREM), and layer-wise reconstruction errors. These results (visualized in Fig. 2. (a)-(c)) underscore neutrino tomography's unique role in geophysical exploration.

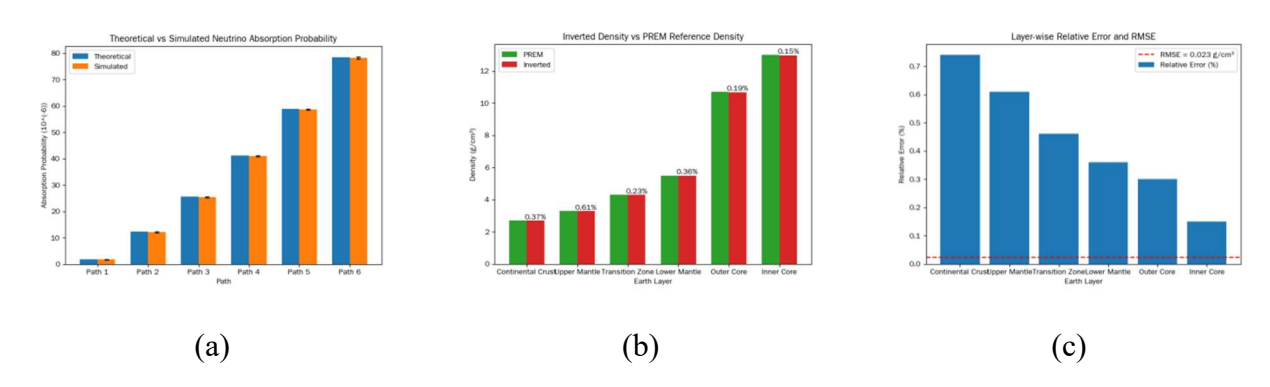


**Fig. 2** (a) Neutrino absorption probability, (b) Density inversion accuracy (vs PREM), (c) Layerwise reconstruction errors.

# 3.5 Analysis of Accuracy

The analysis of accuracy reveals strong overall consistency between the inverted densities and the PREM model, with a maximum relative error of 0.67% (observed in the transition zone), validating the efficacy of neutrino tomography for probing Earth's internal structure. Notably, the inner core exhibits the smallest relative error (0.15%), underscoring neutrino tomography's unique advantage in penetrating high-density regions-such as the outer core, which is inaccessible to shear waves in traditional seismic methods. The RMSE of approximately 0.023 g/cm³ further confirms the method's reliability, demonstrating that neutrino-based density inversion provides robust and precise results.

# 4. Discussion

The results of this study demonstrate that neutrino tomography, utilizing artificial neutrino beams, offers a robust and precise method for probing Earth's internal structure, complementing traditional seismic techniques. The close agreement between inverted densities and the PREM model-with a maximum relative error of 0.67% and an RMSE of ~0.023 g/cm³-validates the feasibility of this approach.

A key advantage of neutrino tomography lies in its ability to penetrate the entire Earth, including the liquid outer core, which is inaccessible to S-waves in seismic tomography. This is reflected in the low relative error of 0.30% for the outer core and 0.15% for the inner core, highlighting the method's unique capability to constrain density in high-pressure, high-density regions that are critical to understanding Earth's formation and dynamics.

The use of artificial neutrino beams represents a critical innovation. Unlike natural neutrinos (e.g., from the Sun or atmosphere), which have fixed energy ranges and unpredictable trajectories, artificial beams allow controlled tuning of energy and direction. This control enables targeted probing of specific layers (e.g., the transition zone via Path 3) and enhances resolution by optimizing interaction probabilities through energy adjustment.

However, the study has limitations that warrant consideration. The Earth is modeled as a perfect sphere, whereas its actual oblate shape and variable crustal thickness (e.g., thinner oceanic crust) may introduce minor path length errors. Additionally, the simulation uses a constant neutrino energy (10 GeV), while varying energies could improve sensitivity to different density ranges. Future work should incorporate a more realistic Earth model (e.g., oblate spheroid geometry) and explore multi-energy beam designs to refine layer-specific density constraints.

Another avenue for improvement is addressing stochasticity in neutrino survival measurements. While 1,000 Monte Carlo iterations with 10,000 neutrinos per path ensured statistical stability, increasing sample size or incorporating energy-dependent flux variations could further reduce uncertainties, particularly for layers with small absorption probabilities (e.g., the crust, with  $P_{\rm abs} \approx 0.0019\%$ ).

# 5. Conclusion

This study presents a novel framework for neutrino tomography using artificial neutrino beams to probe Earth's internal structure, addressing key limitations of traditional seismic methods. By simulating neutrino propagation through a six-layer Earth model and inverting survival data to reconstruct densities, the results demonstrate strong agreement with the PREM model, with an RMSE of 0.023 g/cm<sup>3</sup> and maximum relative error of 0.67%.

The method's ability to penetrate the entire Earth-including the liquid outer core-highlights its potential as a complementary tool for geophysical research. The precision of inverted densities, particularly in the inner core (0.15% relative error), validates neutrino tomography as a reliable technique for constraining Earth's deep composition.

Future advancements, including refined Earth models, multi-energy neutrino beams, and larger-scale simulations, will enhance the method's resolution and applicability. Ultimately, neutrino tomography could revolutionize our understanding of Earth's dynamics, with implications for resource exploration, planetary science, and hazard assessment.

# References

- [1] Incorporated Research Institutions for Seismology (IRIS), "Exploring the Earth using seismology," in Education & Outreach Series, no. 5, Washington, DC, USA, 2008. [Online]. Available: https://www.iris.edu/hq/inclass/fact-sheet/exploring\_earth\_using\_seismology
- [2] Incorporated Research Institutions for Seismology (IRIS), "Seismic Shadow Zone: Basic Introduction," [Online].

  Available: https://www.iris.edu/hq/inclass/animation/seismic shadow zone basic introduction.
- [3] M. Paulatto, E. E. E. Hooft, K. Chrapkiewicz, B. Heath, D. R. Toomey, and J. V. Morgan, "Advances in seismic imaging of magma and crystal mush," Front. Earth Sci., vol. 10, pp. 1–8, Oct. 2022, doi: 10.3389/feart.2022.970131.
- [4] A. Donini, S. Palomares-Ruiz, and J. Salvado, "Neutrino Tomography of Earth," Nature Physics, vol. 15, no. 1, pp. 37–40, Jan. 2019, doi: 10.1038/s41567-018-0319-1.
- [5] A. M. Dziewonski and D. L. Anderson, "Preliminary reference Earth model," Phys. Earth Planet. Inter., vol. 25, no. 4, pp. 297-356, Jun. 1980. Available: https://doi.org/10.1016/0031-9201(81)90046-7.
- [6] A. Matsuyama, M. Arai, and T. Sato, "Dynamical coupled-channel model of meson production reactions in the nucleon resonance region," Phys. Rep., vol. 439, no. 4, pp. 193–253, Feb. 2007. Available: https://doi.org/10.1016/j.physrep.2006.12.003.

DOI: 10.6919/ICJE.202510\_11(10).0019

- [7] K. J. Krishnamoorthi, A. K. Upadhyay, A. Kumar, and S. K. Agarwalla, "Probing Earth's core using atmospheric neutrino oscillations with NSI," J. High Energy Phys., 2025. [Online]. Available: arXiv.
- [8] IceCube Collaboration, "The IceCube Neutrino Observatory: Instrumentation and Online Systems," arXiv preprint, 2016. [Online]. Available: https://arxiv.org/abs/1612.05093.
- [9] \*HEPData Search: Elastic Scattering at 7.0-8.0 TeV\*. [Online]. Available: https://www.hepdata.net/search/?q=elastic+scattering&page=1&cmenergies=7.0,8.0&size=50&observa bles=SIG&phrases=Charged+Current&subject\_areas=hep-ex.
- [10] Physics Stack Exchange. "Neutrino cross section approximation." [Online]. Available: https://physics.stackexchange.com/questions/737179/neutrino-cross-section-approximation.